

RESEARCH

Open Access



Gut bacteria *Prevotellaceae* related lithocholic acid metabolism promotes colonic inflammation

Liping Chen^{1†}, Zhenghao Ye^{1,2†}, Junhua Li^{3†}, Lijia Wang¹, Yu Chen¹, Meiping Yu¹, Jian Han¹, Jiangeng Huang⁴, Dongyan Li⁵, Yongling Lv⁶, Kai Xiong⁶, De'an Tian¹, Jiazhi Liao¹, Ursula Seidler² and Fang Xiao^{1*} 

Abstract

Background The conversion of primary bile acids to secondary bile acids by the gut microbiota has been implicated in colonic inflammation. This study investigated the role of gut microbiota related bile acid metabolism in colonic inflammation in both patients with inflammatory bowel disease (IBD) and a murine model of dextran sulfate sodium (DSS)-induced colitis.

Methods Bile acids in fecal samples from patients with IBD and DSS-induced colitis mice, with and without antibiotic treatment, were analyzed using ultraperformance liquid chromatography-mass spectrometry (UPLC-MS). The composition of the microbiota in fecal samples from IBD patients and DSS-colitis mice was characterized via Illumina MiSeq sequencing of the bacterial 16S rRNA gene V3-V4 region. Metagenomic profiling further identified metabolism-related gene signatures in stool samples from DSS-colitis mice. Histological analysis, quantitative PCR (qPCR) and Western Blotting were conducted on colonic samples from DSS-induced colitis mice to assess colonic inflammation, mucosal barrier integrity, and associated signaling pathways. The multivariate analysis of bile acids was conducted using Soft Independent Modelling of Class Analogy (SIMCA, Umetrics, Sweden). The relation between the relative abundance of specific phyla/genera and bile acid concentration was assessed through Spearman's correlation analyses. Finally, lithocholic acid (LCA), the key bile acid, was administered via gavage to evaluate its effect on colonic inflammation and mucosal barrier integrity.

Results In patients with IBD, the composition of colonic bile acids and gut microbiota was altered. Moreover, changes in the gut microbiota further modulate the composition of bile acids in the intestine. As the gut microbiota continues to shift, the bile acid profile undergoes additional alterations. The aforementioned alterations were also observed in mice with DSS-induced colitis. The study revealed a correlation between dysbiosis of the gut microbiota and modifications in the profile of colonic bile acids, notably LCA observed in both patients with IBD and mice with DSS-induced colitis. Through multivariate analysis, LCA was identified as the key bile acid that significantly affects colonic inflammation and the integrity of mucosal barrier. Subsequent experiments confirmed that LCA supplementation effectively mitigated the inhibitory effects of gut microbiota on colitis progression in mice, primarily through the activation of the sphingosine-1-phosphate receptor 2 (S1PR2)/NF- κ B p65 signaling pathway. Analysis of the microbiome and metagenomic data revealed changes in the gut microbiota, notably an increased abundance

[†]Liping Chen, Zhenghao Ye and Junhua Li contributed equally to this study.

*Correspondence:

Fang Xiao

xiaofang@tjh.tjmu.edu.cn

Full list of author information is available at the end of the article



of an unclassified genus within the family *Prevotellaceae* in DSS-induced colitis mice. Furthermore, a positive correlation was observed between the relative abundance of *Prevotellaceae* and bile acid biosynthesis pathways, as well as colonic LCA level.

Conclusions These findings suggest that LCA and its positively correlated gut bacteria, *Prevotellaceae*, are closely associated with intestinal inflammation. Targeting colonic inflammation may involve inhibiting LCA and members of the *Prevotellaceae* family as potential therapeutic strategies.

Keywords IBD, Colonic bacteria, Bile acid, Lithocholic acid, *Prevotellaceae*

Background

Inflammatory bowel disease (IBD), including Crohn's disease (CD) and ulcerative colitis (UC), is a multifactorial and debilitating disorder [1]. Numerous studies indicate that colonic bacteria play an important role in the formation of colonic inflammation during the colitis development [2]. Notably, areas of the intestine with the greatest bacterial biomass exhibit more pronounced inflammation [3]. Experimental studies have demonstrated that germ-free mice subjected to dextran sulfate sodium (DSS)-induced colitis experience a milder form of the disease compared to normal control mice [4, 5]. Furthermore, the severity of experimental colitis in mice was ameliorated through the manipulation of gut microbiota via broad-spectrum antibiotic treatment [6, 7]. Therefore, understanding the impact of gut microbiota on colonic inflammation is crucial for developing effective interventions to mitigate colitis.

Research has demonstrated gut microbiota-related metabolites are closely linked to colonic inflammation [8]. The regulatory functions of gut microbiota rely on the abundant microbial-related metabolites, such as short-chain fatty acids, lipopolysaccharides and bile acids [9]. Among them, the increasing revelation of the significant role of bile acids in the pathogenesis and progression of colitis is noteworthy [10]. Moreover, notable disparities in colonic microbial-related metabolites between IBD patients and healthy individuals, with a significant alteration in bile acid level observed in the stool of patients with CD and UC patients [10–12].

Bile acid metabolism can be modulated by gut microbiota. Primary bile acids are biosynthesized from cholesterol in the liver, which are subsequently transported to the intestine where specific gut bacteria convert them into secondary bile acids [13]. Abnormal bile acid metabolism has been observed in IBD patients, and the interplay between gut microbiota and bile acids is known to be significant in the development and progression of IBD [12, 14, 15].

Several studies have elucidated the impact of gut microbiota on bile acid metabolism in colitis. Additionally, the regulation of bile acid metabolism by gut microbiota has been found to influence colonic inflammation.

The deficiency of secondary bile acid induced by dysbiosis has been shown to exacerbate colonic inflammation [14]. Furthermore, gut microbiota-related bile acid metabolism could influence colitis and the response to anti- $\alpha 4\beta 7$ -integrin therapy in colitis mice [16, 17]. Certain compounds, including 5-aminosalicylic acid, Herba Origani and dihydromyricetin, have demonstrated the ability to alleviate DSS-colitis mice through reshaping gut microbiota and regulating bile acid metabolisms [18–20]. The biosynthesis of secondary bile acids required the involvement of bile salt hydrolase enzymes derived from *Bifidobacteriales*, *Lactobacillales*, *Bacteroidales* and *Clostridiales* [21]. Furthermore, the supplementation of these gut bacteria has been shown to ameliorate colitis by modulating the metabolism of bile acid [22]. Thus, protective bacteria hold potential for improving colitis through regulating bile acid metabolism.

However, there is limited knowledge regarding the specific bacteria that promote the development of colitis by modulating bile acid metabolism. Exploring the influence of colonic bacteria on bile acid metabolism in the inflamed intestine may provide insights into the pathogenesis of IBD and identify potential therapeutic targets. This study aimed to investigate the impact of gut microbiota on the composition of colonic bile acid, and determine whether the modification of bile acid pool by dominant bacteria would affect the severity of colonic inflammation in IBD patients and DSS-colitis mice.

Methods

Participants

IBD patients and normal individuals were recruited from participants at Tongji Hospital, Huazhong University of Science and Technology, Wuhan, China for this study. They were divided into five groups, i.e. normal control (NC) group, Crohn's disease without antibiotics administration (CD) group, Crohn's disease with antibiotics administration (CD-A) group, ulcerative colitis without antibiotics administration (UC) group, and ulcerative colitis with antibiotics administration (UC-A) group, as showed in Table 1. IBD clinical classification was assessed according to the Montreal classification system. IBD clinical activity was evaluated by total Mayo

Table 1 Demographics and clinical features of IBD patients

Variables	CD	CD-A	UC	UC-A	NC	P
Gender, n						0.053
Male	11	10	9	10	15	
Female	1	2	10	9	10	
Age, y	37±11	35±13	47±14	49±16	41±17	0.058
Total Mayo scores			9.1±1.9	10.1±2.3		0.181
CDAI	203±96	227±86				0.527
SES-CD	4.6±1.5	5.5±1.4				0.134
Montreal classification, n (%)						
UC extent						0.830
E1 Proctitis			2	1		
E2 Left-sided colitis			5	5		
E3 Extensive colitis			12	13		
Age at diagnosis (A)						0.543
A1 16 years or younger	1	1				
A2 17–40 years	8	10				
A3 Over 40 years	3	1				
Location (L)						0.435
L1 Terminal ileum	5	7				
L2 Colon	1	2				
L3 Ileocolon	6	3				
L4 Upper GI	0	0				
Behaviour (B)						0.514
B1 Nonstricturing, nonpenetrating	4	3				
B2 Stricturing	8	7				
B3 Penetrating	0	2				
P Perianal disease modifier	5	4				

CD Crohn's disease without antibiotics administration group, CD-A Crohn's disease with antibiotics administration group, UC ulcerative colitis without antibiotics administration group, UC-A ulcerative colitis with antibiotics administration group, NC normal control group, CDAI Crohn's disease activity index, SES-CD simple endoscopic score for Crohn's disease

scores for UC patients, and Crohn's disease activity index (CDAI) and simple endoscopic score for Crohn's disease (SES-CD) for CD patients [23, 24]. Fecal samples were collected for bacteria and targeted metabolomics of bile acids analysis. IBD diagnosis was established on the basis of conventional clinical, radiological, endoscopic and histological findings according to European Crohn's and Colitis Organisation guidelines [25]. Written informed consents were obtained from participants. The study was conducted following the Declaration of Helsinki and approved by the Ethical Committee of Tongji Hospital (TJ-C20161201).

Animals and experimental procedures

6-week-old C57BL/6 female mice were obtained from the Tongji Laboratory Animal CO. LTD (Tongji Laboratory Animal Center, Tongji hospital) and adapted to environmental conditions for one week before experiments. All the animal experiments were approved by the Animal Care and Use Committee of Tongji Hospital, Huazhong

University of Science and Technology (TJ-A20161212). Acute colitis was induced by treating the animals with 3% w/v DSS (36–50 kDa, MP Biomedicals, Solon, OH, USA), given in the drinking water, for 7 days. Simultaneously, different kinds of antibiotics were administered in three different groups, respectively, i.e. ceftriaxone sodium (CRO, 100 mg/kg, Roche, given by gavage) as mostly anti-Gram-negative bacteria [26], vancomycin (VA, 100 mg/kg, Hisun, given by gavage) as mostly anti-Gram-positive bacteria [27], and VA + imipenem (IPM, 100 mg/kg, Merck, given by intraperitoneal injection) as broad-spectrum antibiotics, as described in previous studies [28]. To study the effect of LCA, LCA (250 mg/kg, 376.57 Da, Yuanye Biotechnology Ltd., Shanghai, China) were given by gavage when DSS or DSS + VA + IPM administered simultaneously. On the 8th day, the mice were sacrificed via intraperitoneal injection of a lethal dose of sodium pentobarbital. Then the full colons and fecal material were collected and stored in a freezer at – 80 °C. The remains were collected in plastic biohazard

bags and subsequently stored in the designated animal carcass freezer for standardized disposal by specialized waste management personnel.

DAI and histological analysis

Mice were weighed and assessed for diarrhea and rectal bleeding daily. The disease activity index (DAI) was scored according to the criteria previously described by Sann et al. [29]. Colonic samples after formalin-fixed and paraffin-embedded were sectioned and hematoxylin and eosin-stained in standard procedures. The sections were graded blindly by three pathologists. The colitis was histologically graded on a scale as used in previous study [30].

Isolation of RNA and qPCR

Total RNA was isolated from colon tissues and cells using TRIzol reagent according to the manufacturer's protocol (Invitrogen, Carlsbad, CA, USA). One microgram of RNA was used for cDNA synthesis with the PrimeScript RT reagent Kit (TaKaRa, Dalian, China) for quantitative PCR on an ABI StepOne Real-Time PCR System (Applied Biosystems, Carlsbad, CA, USA) in the presence of the fluorescent dye SYBR Mix (GeneCopoeia, Rockville, MD, USA). The procedures were performed following a three-step method for programming the PCR reaction: 95 °C initial denaturation for 10 min; 95 °C denaturation for 10 s, 60 °C annealing for 20 s, 72 °C extension for 15 s for 40 cycles; and melting curve analysis. The value of $2^{-\Delta\Delta C_t}$ was used to determine fold differences between samples with normalization to GAPDH expression. The primers used were designed according to NCBI Primer-BLAST, and the primer sequences are presented in Supplementary Table 1.

Western Blot

The proteins were extracted from colon tissue using the Protein Extraction Kit according to the manufacturer's protocol (Beyotime, Haimen, China). The protein concentration was determined with a BCA Protein Assay Kit (Beyotime, Haimen, China). For performing Western Blot, 30 μ g proteins were separated on a 12% SDS-PAGE gel. The blotted membranes were blocked with 5% non-fat dried milk in TBST for 1 h at room temperature and then incubated at 4°C with each primary antibody overnight. Anti- β -Actin (1:1000), ZO-1 (1:1000), Occludin (1:1000) and NF- κ B p65 (1:1000) were purchased from Abcam, USA. The membranes were washed and incubated with HRP-labelled goat anti-mouse IgG (1:10,000) or HRP-labelled goat anti-rabbit IgG (1:10,000) for 1 h. The immunoreactive bands were visualized by enhanced chemiluminescence using a Beyo ECL Plus Kit (Beyotime, Haimen, China). Western blot bands were scanned

and analyzed using the ImageJ analysis software package (NIH).

Targeted metabolomics of bile acids

Bile acids in feces from participants and mice were analyzed by ultraperformance liquid chromatography-mass spectrometry (UPLC-MS) as previously reported [31]. Briefly, bile acids were extracted with 70% ethanol at 55 °C for 4 h and then subjected to solid-phase extraction using solid-phase extraction technique [UCT-Clean-Up C18 (Chromatographic Specialties Inc., Brockville, ON, Canada); Oasis-HLB and Oasis-MAX cartridges (Waters Corporation, Milford, MA)]. The resultant residue was redissolved in 100 mL of methanol and centrifuged at 18,000 rpm for 10 min. Chromatography was performed on a Shimadzu HPLC system (Kyoto, Japan) coupled to an AB SCIEX 4000 mass spectrometer (Applied Biosystems, MDS; SCIEX, Framingham, MA). A Waters Atlantis T3 column (2.1 \times 100 mm, 3 mm) protected by a Security Guard (Phenomenex Inc., Torrance, CA) was used for chromatographic separation. The mobile phase consisted of 0.1% formic acid in water and methanol. d4-CA was used as internal standards. Fourteen bile acids were detected including cholic acid (CA), chenodeoxycholic acid (CDCA), taurocholic acid (TCA), taurochenodeoxycholic acid (TCDCA), beta-muricholic acid (β MCA), tauro-alpha-muricholic acid (T α MCA), tauro-beta-muricholic acid (T β MCA), deoxycholic acid (DCA), lithocholic acid (LCA), ursodeoxycholic acid (UDCA), taurodeoxycholic acid (TDCA), tauroolithocholic acid (TLCA), ursocholic acid (UCA), hyodeoxycholic acid (HDCA) in the fecal samples of patients. Fourteen bile acids were detected including CA, CDCA, TCA, TCDCA, alpha-muricholic acid (α MCA), β MCA, T α MCA, T β MCA, DCA, LCA, UDCA, TDCA, TLCA, tauroursodeoxycholic acid (TUDCA) in the mouse fecal samples.

16S rRNA sequencing and bacteria analysis

Amplicons were extracted from 2% agarose gels, purified via the AxyPrep DNA Gel Extraction Kit (Axygen Biosciences, Union City, CA, USA), and quantified by QuantiFluorTM-ST (Promega BioSciences LLC, Sunnyvale, CA, USA) according to the manufacturer's protocols. Then, purified amplicons were pooled and paired-end sequenced (2 \times 300) on an Illumina MiSeq platform (Illumina Inc., San Diego, CA, USA) according to the standard instructions. All raw reads were screened according to barcode and primer sequences, through Quantitative Insights Into Microbial Ecology (QIIME, version 1.17), with the following criteria: (1) The 300 bp reads were truncated at any site receiving an average quality score < 20 over a 10 bp sliding window; (2) the truncated

reads which were shorter than 50 bp were abandoned; (3) Sequences that overlap < 10 bp, or > 2 nucleotide mismatch in primer matching, or reads containing ambiguous characters were removed. Operational taxonomic units (OTUs) were clustered with the cut-off value of 97% similarity using UPARSE (version 7.1, <http://drive5.com/uparse/>), and UCHIME was used to identify and remove chimeric sequences. RDP Classifier (<http://rdp.cme.msu.edu/>) was used to analyze the phylogenetic affiliation of the 16S rRNA gene sequence, against the Silva (version 138.1) 16S rRNA database with a confidence threshold of 70%.

Metagenomic sequencing

Total genomic DNA was extracted from mice fecal samples via the E.Z.N.A.[®] Soil DNA Kit (Omega Bio-tek, Norcross, GA, U.S.) according to the standard instructions. DNA extract was fragmented to an average size of about 400 bp using Covaris M220 (Gene Company Limited, China) for paired-end library construction. Paired-end library was built by NEXTFLEX[™] Rapid DNA-Seq (Bio Scientific, Austin, TX, USA). Adapters which contained the full complement of sequencing primer hybridization sites were ligated to the blunt-end of fragments. Paired-end sequencing was executed on Illumina NovaSeq/HiSeq X ten (Illumina Inc., San Diego, CA, USA) at Majorbio Bio-Pharm Technology Co., Ltd. (Shanghai, China) using NovaSeq Reagent Kits/HiSeq X Reagent Kits according to the standard protocols (www.illumina.com). Finally, 47.7 Gb of high-quality PE reads for the 15 samples were acquired with an average of 3.2 Gb per sample. Sequence data have been deposited in the NCBI Short Read Archive database, <https://www.ncbi.nlm.nih.gov/bioproject/1161371>. Open reading frames (ORFs) in contigs were confirmed by MetaGene (<http://metagene.cb.k.u-tokyo.ac.jp/>). The predicted ORFs with length ≥ 100 bp were retrieved and translated into amino acid sequences via the NCBI translation table (<http://www.ncbi.nlm.nih.gov/Taxonomy/taxonomyhome.html/index.cgi?chapter=tgencodes#SG1>). A non-redundant gene catalog was established by CD-HIT (<http://www.bioinformatics.org/cd-hit/>, version 4.6.1) with 90% coverage and 90% sequence identity. Qualified reads were mapped to the non-redundant gene catalog with 95% identity using SOAPaligner (<http://soap.genomics.org.cn/>, version 2.21), and gene abundance in each sample were assessed. Representative sequences of non-redundant gene catalog were annotated based on the NCBI NR database by blastp as implemented in Diamond (<http://www.diamondsearch.org/index.php>, version 0.8.35) with e-value cutoff of $1e^{-5}$ for taxonomic annotations. Cluster of orthologous groups of proteins (COG) annotation for the representative sequences

were implemented by Diamond against eggNOG database (version 4.5.1) with an e-value cutoff of $1e^{-5}$. The KEGG annotation was performed via Diamond against the Kyoto Encyclopedia of Genes and Genomes database (<http://www.genome.jp/kegg/>, version 94.2) with an e-value cutoff of $1e^{-5}$.

Statistical analysis

Statistical analyses were performed with SPSS 21.0 (SPSS, Inc., Chicago, IL, USA) and GraphPad Prism (version 8.01, GraphPad Prism Inc., USA). Results are expressed as mean \pm standard deviation (S.D.). Data among groups were evaluated by one-way ANOVA or two-way ANOVA, followed by Tukey's post-test. The Mann-Whitney U test was used to examine differences in bacterial composition between the two groups. The multivariate data analysis of bile acids was carried out using Soft Independent Modelling of Class Analogy (SIMCA, Umetrics, Sweden) and variable importance in projection (VIP) analysis was used to investigate which bile acids distinguish these groups [32]. The relation between the relative abundance of certain phylum/genus and bile acids concentration was performed by Spearman's correlation analyses. Spearman's correlation analyses were also used to assess the changes of 8 types of bile acid biosynthesis pathway genes and the relative abundance of top 20 genera among the five groups. A two-side $P < 0.05$ was considered to be statistically significant.

Results

Altered bile acid composition and colonic microbiota in IBD patients.

The demographic characteristics of the participants were presented in Table 1. There were no significant differences in gender and age among the groups classified as NC, UC, UC-A, CD, CD-A. Furthermore, the clinical features, Montreal classification and total Mayo scores for UC, as well as Montreal classification, CDAI and SES-CD for CD, were not significantly different between UC group and UC-A group or between CD group and CD-A group.

Principal component analysis (PCA) was performed to examine the distribution of fecal bile acids among the five groups (Fig. 1A). A distinct separation was observed between NC group and IBD groups. Additionally, a discernible distinction in bile acid composition was observed between UC group and UC-A group, as well as CD group and CD-A group (Fig. 1A). Furthermore, an orthogonal partial least squares discriminant analysis (OPLS-DA) model displayed that the samples from each group clustered closely together (Fig. 1B). There were notable differences observed in various bile acids between IBD patients and normal control. Furthermore,

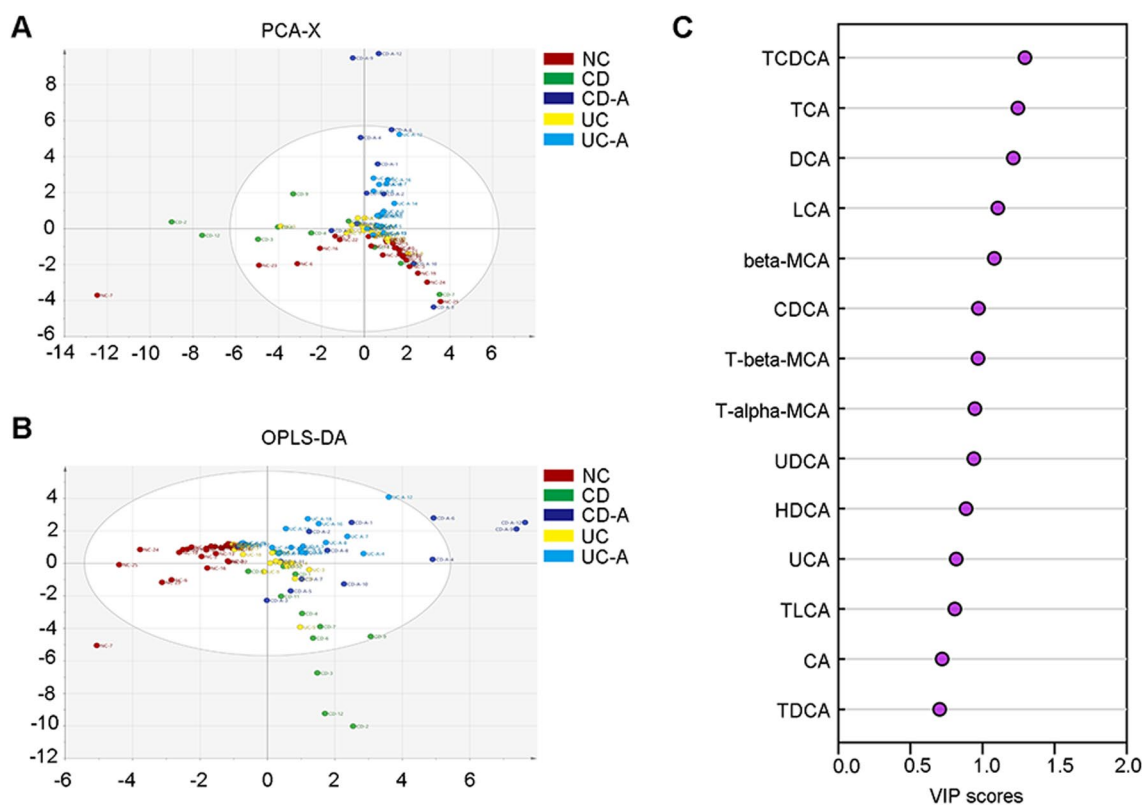


Fig. 1 Multivariate analysis of bile acid profiling data for participants. **A** PCA scores plot. **B** OPLS-DA scores plot. **C** Variable importance in projection (VIP) plot identified by OPLS-DA displaying the bile acids. NC normal control group, CD Crohn's disease without antibiotics administration group, CD-A Crohn's disease with antibiotics administration group, UC ulcerative colitis without antibiotics administration group, UC-A ulcerative colitis with antibiotics administration group, PCA principal component analysis, OPLS-DA orthogonal partial least squares-discriminant analysis

the administration of antibiotics to modulate the microbiota resulted in alterations in certain bile acids (SFigure 1). The overall contribution of each bile acid was assessed using the variable importance in the projection (VIP) method (Fig. 1C). Notably, the bile acids TCDCA, TCA, DCA, LCA and β MCA were identified significantly different among the five groups when the VIP threshold was set to 1. These findings indicated the five bile acids possessed the highest predictive power.

At the phylum level, the dominant phyla of the five groups were *Firmicutes*, *Proteobacteria*, *Bacteroidetes*, *Actinobacteria* and *Fusobacteriota* (Fig. 2A). The UC group and the CD group exhibited significantly lower relative abundance of *Bacteroidetes* compared to the NC group, while the UC group and the CD group showed significantly higher relative abundance of *Proteobacteria* compared to the control group. At the genus level, the UC group and the CD group displayed lower relative abundance of *Bacteroides* compared to the NC group, and this relative abundance was further reduced after antibiotics administration (Fig. 2B). Similar changes in

the gut microbiota could be detected at the class, order, family and species levels (SFigure 2).

Modulation of gut microbiota attenuates the severity of DSS-colitis in mice

Colon length was shorter in the DSS-colitis mice compared to controls, with a partial recovery after modulation of gut microbiota by antibiotics co-administration (Fig. 3A, B). The DAI and histological score were improved in DSS-colitis mice co-administrated with antibiotics as compared to the DSS-colitis mice without antibiotics (Fig. 3C–E). The mRNA expression of pro-inflammatory factors TNF- α , IL-1 β and IFN- γ in colon tissues was elevated enormous times as 9.4, 14.6, 11.0, respectively after DSS administration and the increase was suppressed when the microbiota were modulated by antibiotics treatment (Fig. 3F–H). The protein expression levels of ZO-1 and occludin were markedly decreased in the colitis mice compared to controls, with a partial restoration with antibiotics co-administration (Fig. 3I–K). The findings indicated that, a partial recovery of the

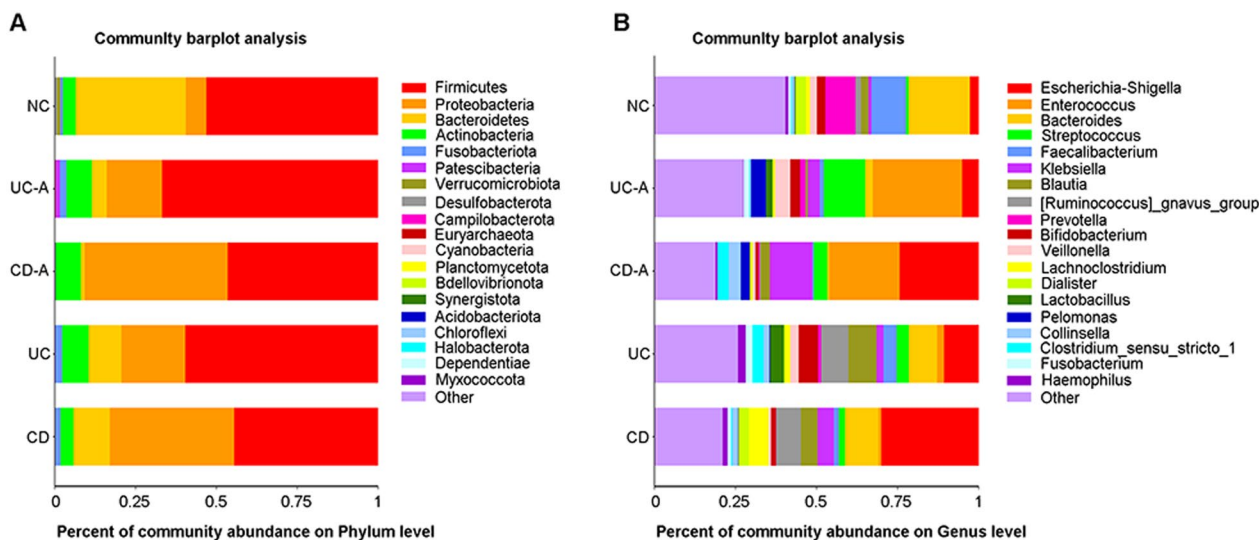


Fig. 2 Changes in microbiota abundance in feces of patients. **A** Community bar-plot analysis shows relative abundance of microbiota in fecal samples of five groups at the phylum level. **B** Community bar-plot analysis shows relative abundance of microbiota in fecal samples of five groups at the genus level. Statistical analysis was performed with one-way ANOVA followed by with Tukey's post-test. NC normal control group, UC-A ulcerative colitis with antibiotics administration group, CD-A Crohn's disease with antibiotics administration group, UC ulcerative colitis without antibiotics administration group, CD Crohn's disease without antibiotics administration group

colitis was observed in DSS-colitis mice after modulation of gut microbiota by antibiotics co-administration.

LCA has the most predictive power on colonic inflammation in DSS-colitis mice

A clear separation was observed among NC group, DSS group and DSS+antibiotics groups by PCA (Fig. 4A). The OPLS-DA model demonstrated that the samples within each group exhibited a high degree of clustering. (Fig. 4B). Compared with the control group, the levels of α MCA, UDCA, β MCA, TLCA, CA were increased significantly, and the level of DCA was decreased significantly in DSS group (SFigure 3). In comparison to the DSS group, the modulation of microbiota through antibiotic administration in DSS-colitis mice resulted in a significant elevation of taurine-associated bile acids T β MCA, TCA, and TUDCA, while concurrently leading to a reduction in secondary bile acids LCA, UDCA,

TDCA, TLCA, and DCA (SFigure 3). As shown in Fig. 4C, the predominant bile acids LCA was chosen when VIP threshold of 2.5 was used. It indicated the LCA had the most predictive power on the colitis severity.

Gut bacteria play an important role in bile acid metabolism in DSS-colitis mice

At the phylum level (Fig. 5A), the dominant phyla of the five groups were *Firmicutes*, *Bacteroidetes*, *Proteobacteria*, *Tenericutes* and *Epsilonbacteraeota*. The relative abundance of *Firmicutes* was the highest in the five groups. The relative abundance of *Bacteroidetes* was reduced after antibiotics administration. At the genus level (Fig. 5B), the relative abundance of *Lactobacillus* was highest in the NC group, and the relative abundance of *Lactobacillus* were significantly lower in the DSS group, DSS+CRO group and DSS+VA+IPM group, except for DSS+VA group. At the class, order, family

(See figure on next page.)

Fig. 3 Changes in DSS-colitis severity and mucosal barrier damage. **A** Representative images showing the gross appearance of colons of five groups. **B** Colon length at sacrifice. **C** The changes in DAI, scored in terms of body weight loss, stool consistency, and bleeding. **D** HE-stained colon sections of mice (original magnification $\times 100$ and $\times 200$). Scale bar: 40 μ m (upper panels), 20 μ m (lower panels). **E** Histological scores of tissues from mice of five groups. **F, G, H** Relative mRNA expression of TNF- α , IL-1 β , IFN- γ from mice of five groups. **I, J, K** Colonic expression of tight-junction protein ZO-1 and OCLN were assessed by western blot. NC normal control group, DSS colitis induced by treating with dextran sulfate sodium (DSS) group, DSS+CRO treated with DSS and ceftriaxone sodium group, DSS+VA treated with DSS and vancomycin group, DSS+VA+IPM treated with DSS, vancomycin and imipenem group, TNF- α tumor necrosis factor alpha, IL-1 β Interleukin 1 beta, IFN- γ interferon gamma, ZO-1 zonula occludens-1, OCLN occludin. The relative grey value was used to quantify ZO-1 and OCLN protein expression. Statistical analysis was performed with one-way or two-way ANOVA with Tukey's post-test versus NC group. * $P < 0.05$, ** $P < 0.01$, *** $P < 0.001$, versus DSS group. # $P < 0.05$, ## $P < 0.01$, ### $P < 0.001$

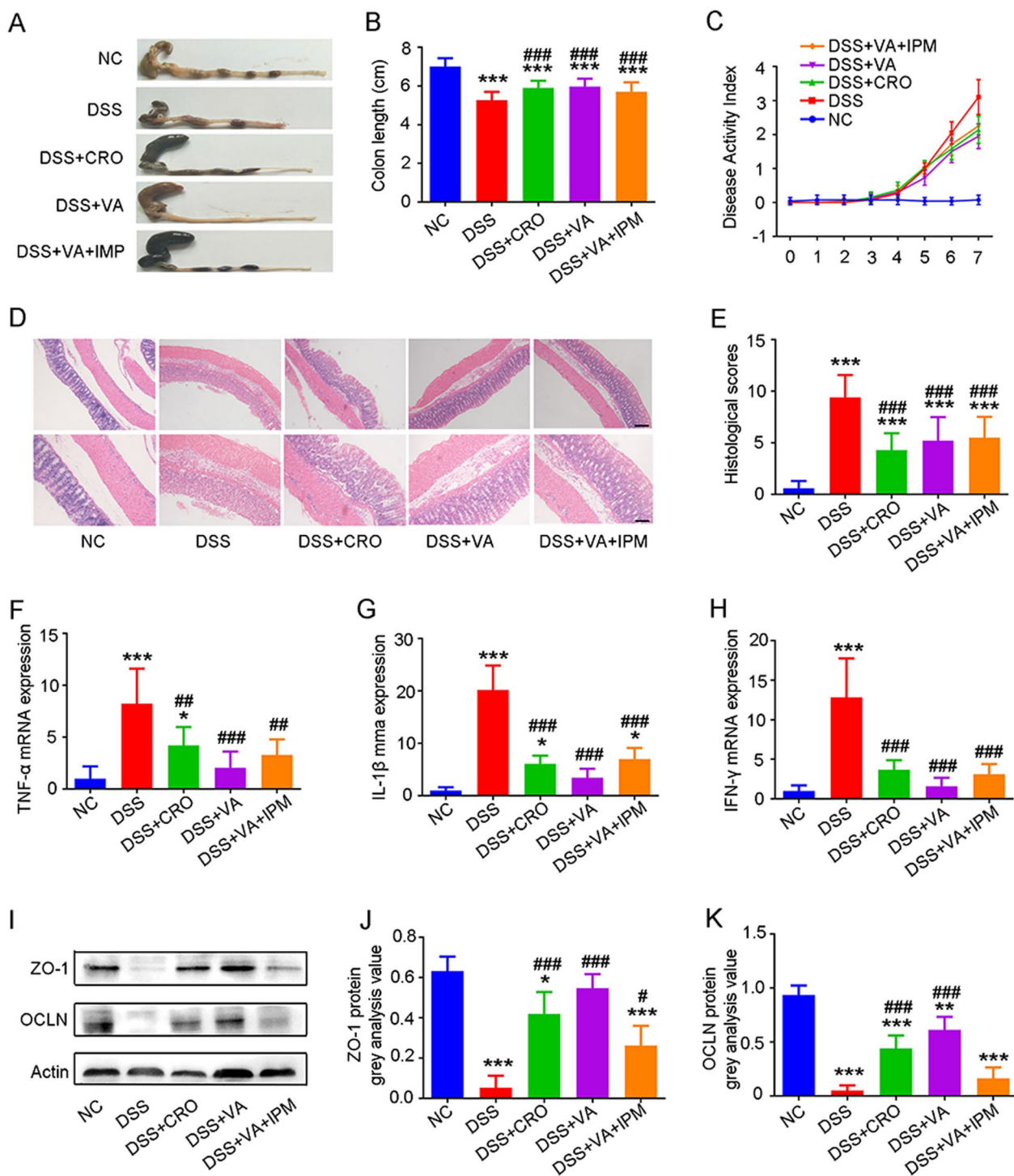


Fig. 3 (See legend on previous page.)

and species levels, similar changes in the gut microbiota could be tested (SFigure 4).

Spearman correlation analysis was carried out in the top 50 genera of relative abundance among the five groups to find out the relation between gut bacteria

and bile acid. The results showed that the rest 48 genera out of the top 50 genera were significantly associated with changes in at least one bile acid, except for the two genera *Romboutsia* and *Eubacterium_fiscatena*. The relative abundance of 31 genera were

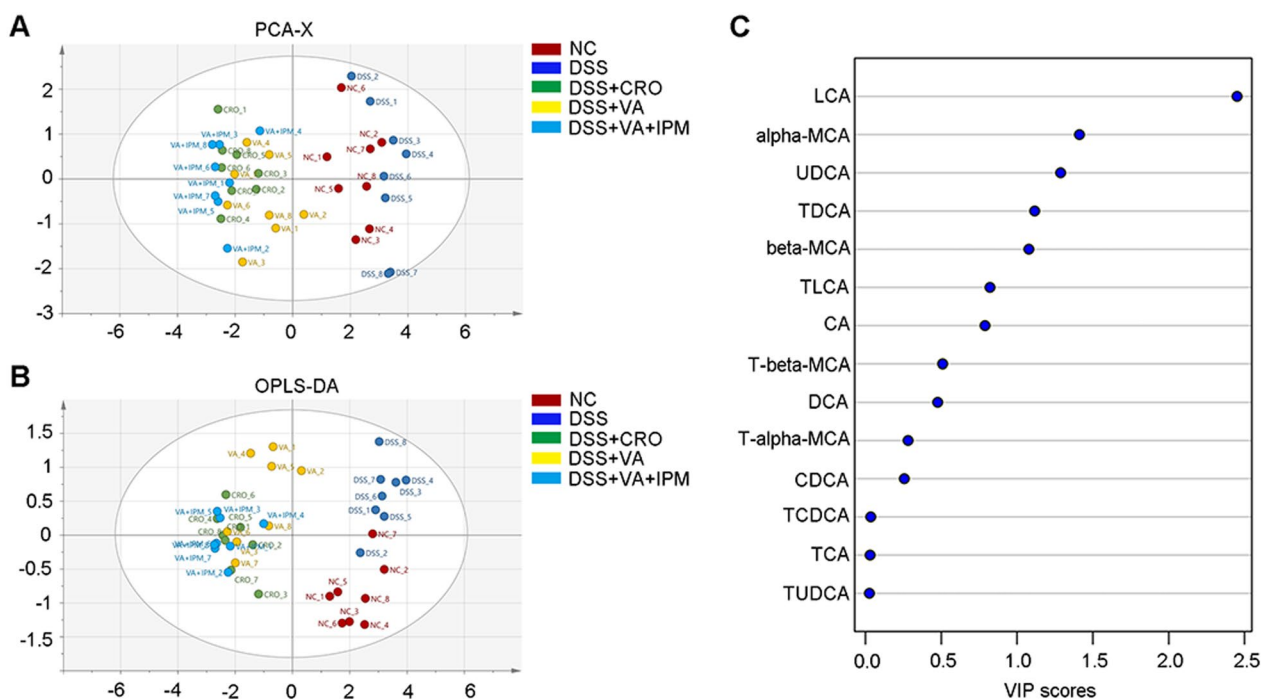


Fig. 4 Multivariate analysis of bile acid profiling data for mice. **A** PCA scores plot. **B** OPLS-DA scores plot. **C** Variable importance in projection (VIP) plot identified by OPLS-DA displaying the 14 kinds of bile acids. *NC* normal control group, *DSS* colitis induced by treating with dextran sulfate sodium (DSS) group, *DSS + CRO* treated with DSS and ceftriaxone sodium group, *DSS + VA* treated with DSS and vancomycin group, *DSS + VA + IPM* treated with DSS vancomycin and imipenem group, *PCA* principal component analysis, *OPLS-DA* orthogonal partial least squares-discriminant analysis

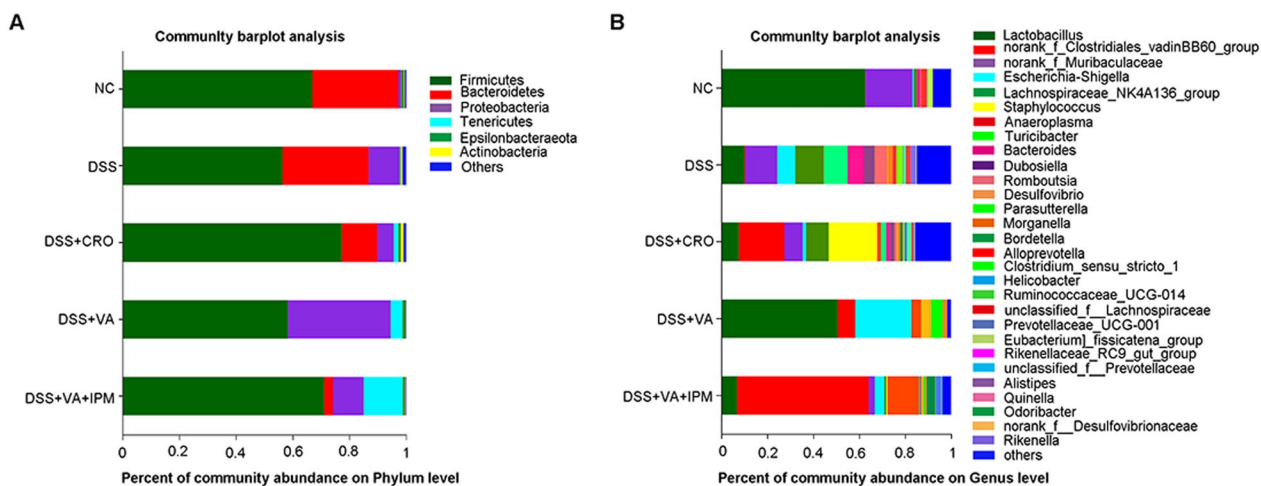


Fig. 5 Changes in microbiota abundance in feces of DSS-colitis mice. **A** Community bar-plot analysis shows relative abundance of microbiota in fecal samples of five groups at the phylum level. **B** Community bar-plot analysis shows relative abundance of microbiota in fecal samples of five groups at the genus level. Statistical analysis was performed with one-way ANOVA with Tukey's post-test. *NC* normal control group, *DSS* colitis induced by treating with dextran sulfate sodium (DSS) group, *DSS + CRO* treated with DSS and ceftriaxone sodium group, *DSS + VA* treated with DSS and vancomycin group, *DSS + VA + IPM* treated with DSS vancomycin and imipenem group

positively correlated with the level of LCA. 6 genera were negatively correlated with the level of LCA (Fig. 6A). The relative abundance of 72, 62, 99 bacterial

genera, respectively, was not significantly different in the CRO, VA and VA + IPM groups, compared to the NC group, respectively. The relative abundance of

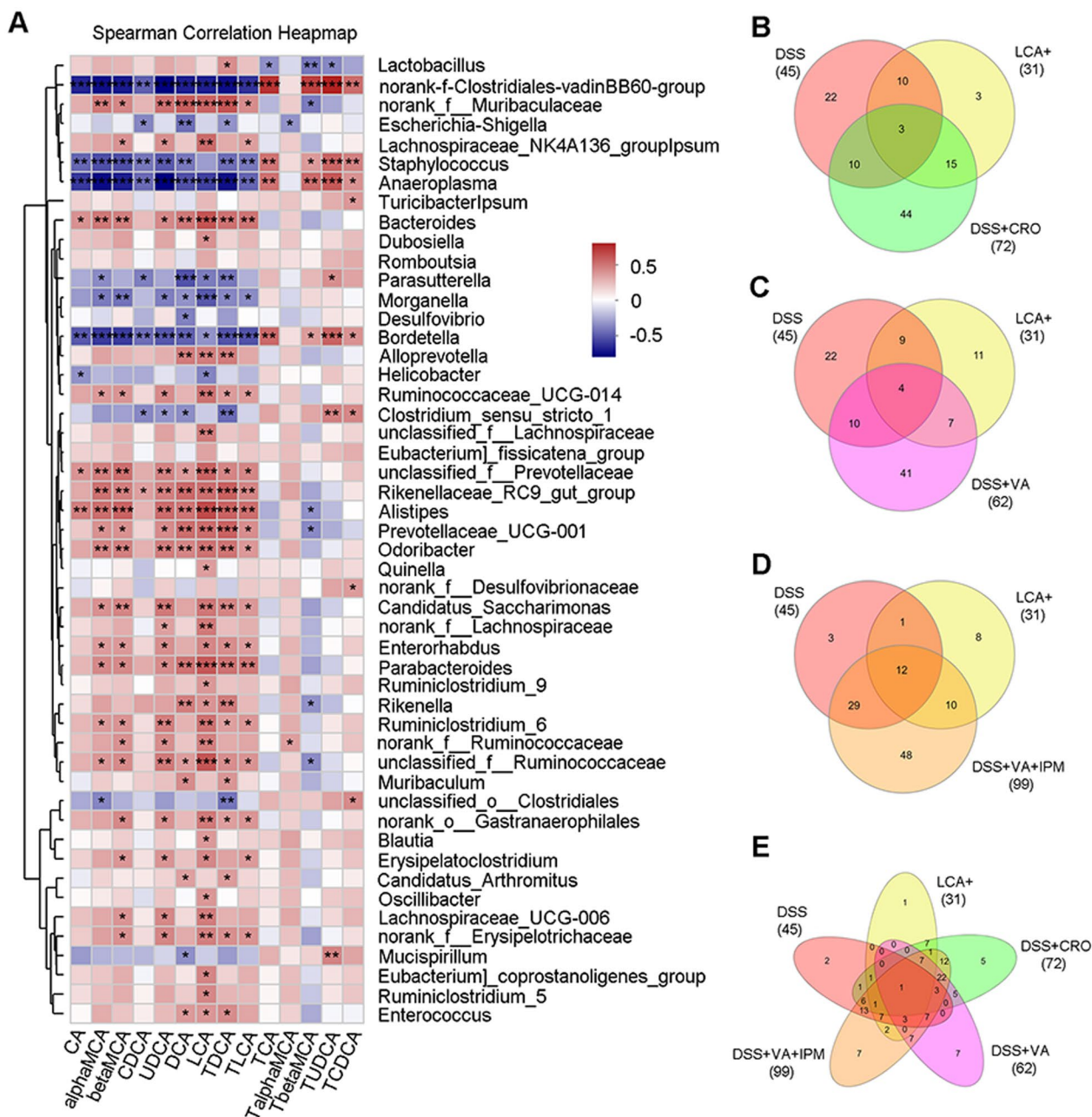


Fig. 6 Correlations between fecal bacteria and metabolome of bile acids. **A** Correlation heatmap of the bile acids and the top fifty genera. **B, C, D, E** Venn diagram showing the bacteria genera that were unique to each group and shared among groups. The cluster number for each component is listed. DSS, the genera of which the relative abundance is higher in DSS group than that in NC group; CRO/VA/VA + IPM, the genera of which the relative abundance in CRO/VA/VA + IPM group are not significantly different with that in NC group; LCA+, The genera of which the relative abundance is positively related to the LCA concentration. *P < 0.05, **P < 0.01, ***P < 0.001

45 genera was increased in the DSS group compared with the NC group. To further look for the LCA-associated bacteria which were increased in DSS-colitis and restored to normal level with antibiotics modification, Venn diagrams further demonstrated

significant overlaps between the genera above and the LCA-positive genera (Fig. 6B-E). Among these overlaps, the genus *unclassified_f_Prevotellaceae* was the only overlap of the five clusters (Fig. 6E). It suggested that LCA level was consistent with the abundance of *unclassified_f_Prevotellaceae*.

Prevotellaceae is positively correlated with bile acid biosynthesis pathways and the colonic LCA level in DSS-colitis mice

The important bile acid biosynthesis pathway genes included *hdhA*, E3.5.1.24, *baiB*, *baiA*, *baiCD*, *baiF*, *baiH*, *baiI* (Fig. 7A). We focused on the conversion of primary bile acids to LCA. The results showed the major microbial contributor was genus *Prevotella*, which belongs to family *Prevotellaceae* (Fig. 7B). This suggested that *Prevotellaceae* may be particularly active in the conversion of primary bile acids to LCA.

Given the identification of the key bacterium *unclassified_f__Prevotellaceae* in the aforementioned results (Fig. 6E), the focus shifted towards examining the changes in *unclassified_f__Prevotellaceae* across the various groups (Fig. 7C). Notably, the abundance of *unclassified_f__Prevotellaceae* exhibited a significant increase in the DSS group when compared to the NC group. Subsequent administration of antibiotics resulted in a significant decrease in the abundance of *unclassified_f__Prevotellaceae* compared to the DSS group, although no significant difference was observed when compared to the NC group (Fig. 7C). These

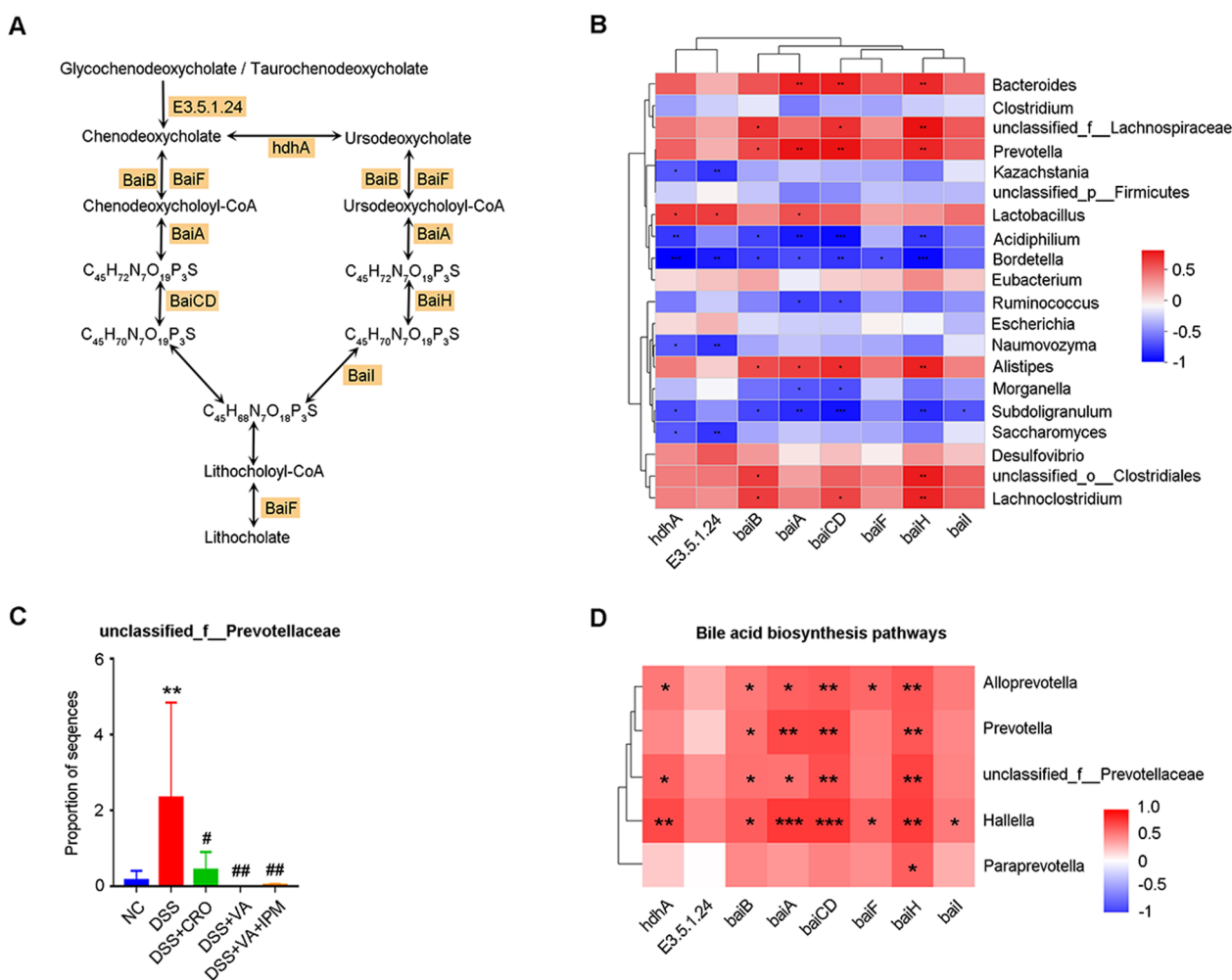


Fig. 7 Effect of *unclassified_f__Prevotellaceae* on colonic LCA. **A** KEGG module for bile acid biosynthesis. **B** Correlations between genera and bile acid biosynthesis associated KOs (red and blue for positive and negative correlation, respectively). Spearman correlation test: * denotes FDR $P < 0.05$; ** denotes FDR $P < 0.01$; *** denotes FDR $P < 0.001$. **C** The proportion of *unclassified_f__Prevotellaceae* in feces of five groups. **D** Correlations between Family *Prevotellaceae* and bile acid biosynthesis associated KOs (red and blue for positive and negative correlation, respectively). NC normal control group, DSS colitis induced by treating with dextran sulfate sodium (DSS) group, DSS + *CRO* treated with DSS and ceftriaxone sodium group, DSS + *VA* treated with DSS and vancomycin group, DSS + *VA* + *IPM* treated with DSS, vancomycin and imipenem group. Spearman correlation test: * denotes FDR $P < 0.05$; ** denotes FDR $P < 0.01$; *** denotes FDR $P < 0.001$. (C) Statistical analysis was performed with one-way ANOVA followed by with Tukey’s post-test versus NC group. * $P < 0.05$, ** $P < 0.01$, *** $P < 0.001$; versus DSS group. # $P < 0.05$, ## $P < 0.01$, ### $P < 0.001$

findings suggested that antibiotic administration had the potential to alter the abundance of *unclassified_f__Prevotellaceae*. Additionally, an assessment of the correlations was conducted between the LCA biosynthesis pathway and the family *Prevotellaceae*, which includes genus *unclassified_f__Prevotellaceae*, *Prevotella*, *Alloprevotella*, *Hallella* and *Paraprevotella* (Fig. 7D). The abundance of *unclassified_f__Prevotellaceae* was positively correlated with the LCA biosynthesis pathway (Fig. 7D). Furthermore, *unclassified_f__Prevotellaceae* was closest to *Prevotella* in family *Prevotellaceae* by cluster analysis (Fig. 7D).

These results suggested that in DSS-colitis mice, the increased abundance of *Prevotellaceae* displayed high expression levels for the genes implicated in the conversion of primary bile acids to LCA, and was associated with an increase in LCA levels Fig. 7A–D).

LCA deteriorates DSS-induced colitis in mice

To further assess the effect of LCA on gut microbiome associated colonic inflammation, LCA was added to DSS-colitis mice as well as DSS-colitis mice with microbiome depletion induced by VA+IPM. The colon length of the mice was significantly shorter (Fig. 8A, B), and the DAI (Fig. 8C) was higher in the DSS+VA+IPM+LCA group compared to the DSS+VA+IPM group. The histological score was significantly lower in the DSS+VA+IPM group comparing with that in the DSS+VA+IPM+LCA group (Fig. 8D, E). The mRNA expression of TNF- α and IFN- γ in colon tissues was decreased after modulating microbiota by antibiotics treatment, but the expression was increased by supply of LCA (Fig. 8F–H). The protein expression levels of ZO-1 and occludin were markedly decreased in DSS+VA+IPM+LCA group than the DSS+VA+IPM group (Fig. 8I–K). These data suggested that antibiotics treatment attenuated the severity of colitis and restores the mucosal barrier, while the effects of antibiotic treatment was repealed after co-administration of LCA on DSS-induced colitis Fig. 8A–K). S1PR2 mRNA expression was significant increase in the mucosal tissue of the DSS group compared with the NC group and modulating microbiota by antibiotics

resulted in a decrease, but supply of LCA abolished the effects of antibiotic treatment (SFigure 5A). The level of NF- κ B p65 was significantly increased in the DSS group than the NC group and could be suppressed after antibiotics treatment (SFigure 5B, 5C), which indicated that the S1PR2/NF- κ B p65 signaling pathway might be involved in the LCA mediated aggravation of DSS-colitis.

Taking together, anti-inflammatory effects of gut bacteria modification, especially *unclassified_f__Prevotellaceae*, in DSS-colitis may be attributed to decreased LCA levels.

Discussion

The findings of this study indicate that *Prevotellaceae* related LCA may play a significant role in the regulation of colonic inflammation. This conclusion is supported by the following observations. (A) The presence of LCA in the stool exhibited alterations in both IBD patients and DSS-colitis mice when compared to the control group. (B) Co-administration of antibiotics during DSS colitis induction ameliorated the colitis, whereas the supplementation of LCA counteracted the anti-inflammatory effect. (C) The abundance of *unclassified_f__Prevotellaceae* exhibited an increase in DSS-colitis mice, but returned to baseline levels following antibiotics administration. (D) The relative abundance of *unclassified_f__Prevotellaceae* displayed a positive correlation with bile acid biosynthesis pathways and the colonic LCA level. Consequently, LCA and its positively related bacteria *unclassified_f__Prevotellaceae* could potentially serve as an intervention target to suppress colonic inflammation.

In our study, LCA was regulated remarkably in DSS-colitis mice after antibiotic administration. Additionally, alterations in gut bacteria were found to induce changes in several types of bile acids. To ascertain the predominant bile acid involved in colitis regulation, VIP followed by OPLS-DA analysis was performed, revealing that LCA played a crucial role in both IBD patients and DSS-colitis mice. It is worth noting that distinct bile acid species exert varying effects on colonic inflammation, with certain bile acids, such as UDCA and DCA, promoting colon repair and alleviating colonic inflammation, while others,

(See figure on next page.)

Fig. 8 The effect of LCA on DSS-induced colitis. **A** Representative images showing the gross appearance of colons of five groups. **B** Colon length at sacrifice. **C** The changes in DAI, scored in terms of body weight loss, stool consistency, and bleeding. **D** HE-stained colon sections of mice (original magnification $\times 100$ and $\times 200$). Scale bar: 40 μ m (upper panels), 20 μ m (lower panels). **E** Histological scores of tissues from mice of five groups. **F, G, H** Relative mRNA expression of TNF- α , IL-1 β , IFN- γ from mice of five groups. **I, J, K** Colonic expression of tight-junction protein ZO-1 and OCLN were assessed by western blot. NC normal control group, DSS colitis induced by treating with dextran sulfate sodium (DSS) group, DSS + VA + IPM treated with DSS, vancomycin and imipenem group, DSS + VA + IPM + LCA treated with DSS, vancomycin, imipenem and lithocholic acid group, DSS + LCA treated with DSS and lithocholic acid group, TNF- α tumor necrosis factor alpha, IL-1 β Interleukin 1 beta, IFN- γ interferon gamma, ZO-1 zonula occludens-1, OCLN occludin. Statistical analysis was performed with one-way or two-way ANOVA with Tukey's post-test versus NC group. * $P < 0.05$, ** $P < 0.01$, *** $P < 0.001$, versus DSS group. # $P < 0.05$, ## $P < 0.01$, ### $P < 0.001$

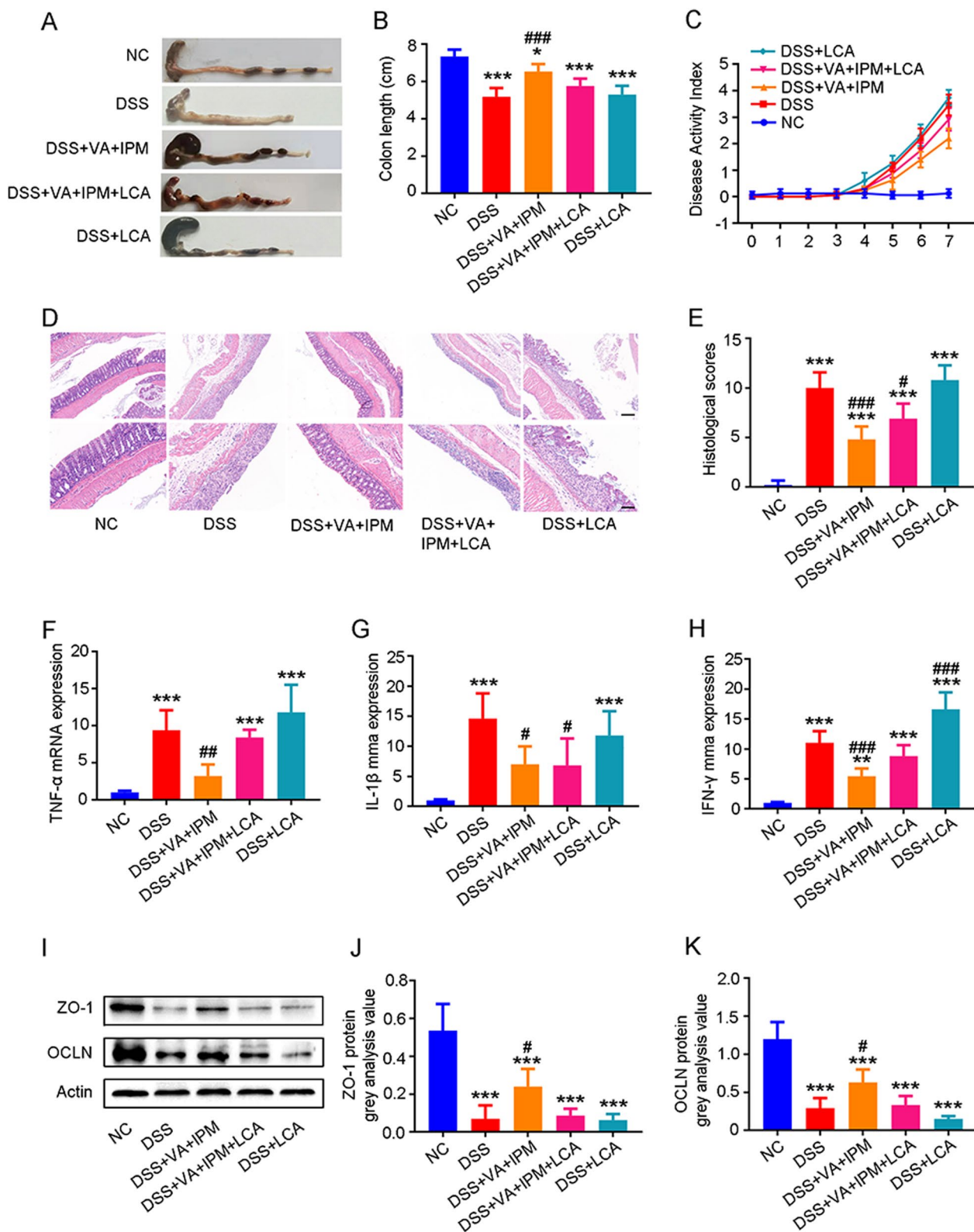


Fig. 8 (See legend on previous page.)

like CA and CDCA, potentially exacerbating it [20, 33, 34]. However, another study revealed that secondary bile acid LCA, when present in low concentrations, exerted an anti-inflammatory effect within the colon by diminishing the levels of pro-inflammatory cytokines [35]. One potential mechanism could involve the perturbation of cell membranes, subsequently activating protein kinase C and releasing arachidonic acid [36], which stimulated the production of inflammatory factors such as TNF- α [37, 38]. S1PR2 was found to be highly expressed in intestinal epithelial cells [39]. In DSS-treated mice, the expression of S1PR2 was upregulated, and colonic inflammation and pathological damage were alleviated by inhibiting S1PR2 [40]. Similarly, our study found that S1PR2/NF- κ B p65 were up-regulated after LCA application in DSS-treated mice.

The gut microbiota plays a crucial role in the onset and development of colonic inflammation [41]. Factors that influence the gut microbiota, such as antibiotics, impact the probability and propagation of IBD [42]. The gut microbiota is now considered to play an essential role in the development and progression of IBD inflammatory. IBD is characterized by decreased microbiota diversity in the gut, altered relative abundances of health-associated taxa and pathobionts, increased numbers of bacteria attaching to the intestinal epithelium [43, 44]. Research has demonstrated that even minor alterations in the microbial community can significantly alter its function [45]. The proliferation of specific pathogenic bacteria, such as *Bacilli*, *Escherichia coli* and *Proteobacteria*, or heightened interaction between the immune system and the normal symbiotic flora, like *Candida albicans*, is considered as triggers for chronic inflammation of IBD [46–49]. Compared with healthy subjects, patients with IBD exhibit a notable decrease in the diversity of their colonic microbiota, and this dysbiosis is often accompanied by an elevation in potentially pathogenic bacteria or a depletion of protective bacteria [50–52]. Furthermore, increased abundance of *Bifidobacterium longum* was found to be related to maintaining remission in CD patients [53]. These findings suggest the potential of utilizing the microbiome as a standalone treatment for IBD. Therefore, it is imperative to investigate the precise mechanisms by which specific bacteria promote colonic inflammation.

This study suggested that *Prevotellaceae* could potentially impact colonic inflammation by modulating the composition of secondary bile acids in the stool. Elinav et al. found that mice deficient in the NLRP6 inflammasome exhibited exacerbated DSS-induced colitis, which was attributed to alteration in the fecal microbiota characterized by an expanded representation of the bacterial family *Prevotellaceae* [54]. Additionally, the deletion

of *Ninjurin1* in mice led to heightened susceptibility to colitis through increasing the abundance of colitogenic *Prevotellaceae* strains and decreasing the presence of immunoregulatory *Lachnospiraceae* strains [55]. Consequently, an increase in the abundance of *Prevotellaceae* may aggravate colitis in mice. Another study proposed that *Kuijieyuan* decoction ameliorated colitis partially by modulating gut microbiota, specifically by increasing the proportions of *Alloprevotella*, *Treponema*, *Prevotellaceae* and *Prevotella*, while reducing the proportions of *Escherichia-Shigella* and *Desulfovibrio* [56]. The relative abundance of *Alloprevotella* significantly decreased following acute DSS induction, and the relative abundance of *Prevotellaceae_UCG-001* significantly decreased following chronic DSS induction [57]. Our study further demonstrated that an increase in the abundance of *unclassified_f_Prevotellaceae* may deteriorate colonic inflammation.

Within the *Bacteroidetes* phylum, *Prevotellaceae* species in stool exhibited a significant correlation with fibrosis-associated and steatosis-associated bile acid parameters [58]. Additionally, *Prevotellaceae* actively participated in the production of short-chain fatty acids [59]. At the genus level, *uncultured_bacterium_f_Prevotellaceae* demonstrated significant correlations with biomarkers related to amino acid and lipid metabolism [60]. Our study provided evidence that an increase in the abundance of *unclassified_f_Prevotellaceae* may exacerbate colonic inflammation by altering the composition of secondary bile acids, particularly by promoting the accumulation of LCA.

Our study further demonstrated the adverse effects of LCA on colonic inflammation. Therefore, the indirect inhibition of LCA by the reduction of gut microbiota composition, especially *unclassified_f_Prevotellaceae*, offers a safer therapeutic approach for managing IBD compared to the direct activation of target pharmacological agents, such as specific bile acids.

Certain limitations need to be taken into account. Firstly, further research is needed to investigate the precise regulatory pathways through which *Prevotellaceae* interacts with LCA. Secondly, additional studies are necessary to explore the regulatory effects of *Prevotellaceae* as an intervention target for colitis.

Conclusions

Altered bile acid composition and colonic microbiota were found in IBD patients. Further, this study has contributed novel insights into the underlying mechanism by which specific bacteria impact secondary bile acid metabolism in DSS-induced colitis. Our findings demonstrate that an unclassified genus within the family *Prevotellaceae* bacteria play a role in promoting colonic

inflammation in mice by the modulation of bile acid LCA metabolite. Consequently, this study suggested that targeting LCA and its positively related bacteria an unclassified genus within the family *Prevotellaceae* could serve as a potential intervention strategy to mitigate colonic inflammation.

Abbreviations

αMCA	Alpha-muricholic acid
βMCA	Beta-muricholic acid
CA	Cholic acid
CD	Crohn's disease
CDAI	Crohn's disease activity index
CDCA	Chenodeoxycholic acid
CRO	Ceftriaxone sodium
DAI	Disease activity index
DCA	Deoxycholic acid
DSS	Dextran sulfate sodium
HDCA	Hyodeoxycholic acid
IBD	Inflammatory bowel disease
IPM	Imipenem
LCA	Lithocholic acid
NC	Normal control
OPLS-DA	Orthogonal partial least squares discriminant analysis
OTU	Operational taxonomic units
PCA	Principal component analysis
S1PR2	Sphingosine-1-phosphate receptor 2
SES-CD	Simple endoscopic score for Crohn's disease
TαMCA	Tauro-alpha-muricholic acid
TβMCA	Tauro-beta-muricholic acid
TCA	Taurocholic acid
TCDCA	Taurochenodeoxycholic acid
TDCA	Taurodeoxycholic acid
TLCA	Taurolithocholic acid
TUDCA	Tauroursodeoxycholic acid
UC	Ulcerative colitis
UCA	Ursocholic acid
UDCA	Ursodeoxycholic acid
UPLC-MS	Ultraperformance liquid chromatography-mass spectrometry
VA	Vancomycin
VIP	Variable importance in the projection

Supplementary Information

The online version contains supplementary material available at <https://doi.org/10.1186/s12967-024-05873-6>.

Supplementary Material 1.
Supplementary Material 2.
Supplementary Material 3.
Supplementary Material 4.
Supplementary Material 5.
Supplementary Material 6.

Acknowledgements

The authors thank pathologists Jun Wang, Ying Wang, Chao Zhang for technical assistance. The authors would like to thank all the subjects who volunteered to participate in this study.

Author contributions

ZY, LC, JL1, LW, YC, MY, JH1, JH2, YL, KX performed experiments; LC, ZY, LW, FX, DL analyzed data; LC, ZY, FX, US wrote the manuscript; ZY, LC, JL1, LW, MY, FX provided human samples; US, DT, JL2, FX supervised parts of the project and made important methodological suggestions; FX designed the study

and obtained funding for the project. All authors read and approved the manuscript.

Funding

This study was supported by the National Natural Science Foundation of China (NSFC) grants 81873556 and 82170546 to FX, China Crohn's & Colitis Foundation (CCCCF) under Grant No. CCCC-QF-2022B67-3 to FX, and Tongji Hospital Fund grant No. 2023B02 to LC.

Availability of data and materials

The datasets used and/or analysed during the current study are available from the corresponding author on reasonable request.

Declarations

Ethics approval and consent to participate

Written informed consents were obtained from participants. The study was conducted following the Declaration of Helsinki and approved by the Ethical Committee of Tongji Hospital (TJ-C20161201). All the animal experiments were approved by the Animal Care and Use Committee of Tongji Hospital, Huazhong University of Science and Technology (TJ-A20161212).

Consent for publication

Not applicable.

Competing interests

The authors declare that they have no competing interests.

Author details

¹Department of Gastroenterology, Tongji Hospital, Tongji Medical College, Huazhong University of Science and Technology, Wuhan, Hubei 430030, People's Republic of China. ²Department of Gastroenterology, Hannover Medical School, Hannover, Germany. ³Department of Nephrology, Tongji Hospital, Tongji Medical College, Huazhong University of Science and Technology, Wuhan, China. ⁴Department of Pharmaceutics, School of Pharmacy, Tongji Medical College, Huazhong University of Science and Technology, Wuhan, China. ⁵Department of Pharmacy, Tongji Hospital, Tongji Medical College, Huazhong University of Science and Technology, Wuhan, China. ⁶Meiyitian Biopharmaceutical (Wuhan) Ltd., Wuhan, China.

Received: 12 June 2024 Accepted: 11 November 2024

Published online: 13 January 2025

References

- Adolph TE, Meyer M, Schwarzler J, Mayr L, Grabherr F, Tilg H. The metabolic nature of inflammatory bowel diseases. *Nat Rev Gastroenterol Hepatol.* 2022;19:753–67.
- Caruso R, Lo BC, Nunez G. Host-microbiota interactions in inflammatory bowel disease. *Nat Rev Immunol.* 2020;20:411–26.
- Wu Y, He Q, Yu L, Pham Q, Cheung L, Kim YS, Wang TTY, Smith AD. Indole-3-carbinol inhibits *Citrobacter rodentium* infection through multiple pathways including reduction of bacterial adhesion and enhancement of cytotoxic T cell activity. *Nutrients.* 2020;12:917.
- Schmidt F, Dahlke K, Batra A, Keye J, Wu H, Friedrich M, Glauben R, Ring C, Loh G, Schaubeck M, et al. Microbial colonization in adulthood shapes the intestinal macrophage compartment. *J Crohns Colitis.* 2019;13:1173–85.
- Llewellyn SR, Britton GJ, Contijoch EJ, Vennaro OH, Mortha A, Colombel JF, Grinspan A, Clemente JC, Merad M, Faith JJ. Interactions between diet and the intestinal microbiota alter intestinal permeability and colitis severity in mice. *Gastroenterology.* 2018;154(1037–1046): e1032.
- Veza T, Molina-Tijeras JA, Gonzalez-Cano R, Rodriguez-Nogales A, Garcia F, Galvez J, Cobos EJ. Minocycline prevents the development of key features of inflammation and pain in DSS-induced colitis in mice. *J Pain.* 2022;24:304–19.

7. Kathania M, Tsakem EL, Theiss AL, Venuprasad K. Gut microbiota contributes to spontaneous colitis in E3 ligase itch-deficient mice. *J Immunol.* 2020;204:2277–84.
8. Lavelle A, Sokol H. Gut microbiota-derived metabolites as key actors in inflammatory bowel disease. *Nat Rev Gastroenterol Hepatol.* 2020;17:223–37.
9. Song X, Sun X, Oh SF, Wu M, Zhang Y, Zheng W, Geva-Zatorsky N, Jupp R, Mathis D, Benoist C, Kasper DL. Microbial bile acid metabolites modulate gut RORgamma(+) regulatory T cell homeostasis. *Nature.* 2020;577:410–5.
10. Vich Vila A, Hu S, Andreu-Sanchez S, Collij V, Jansen BH, Augustijn HE, Bolte LA, Ruigrok R, Abu-Ali G, Giallourakis C, et al. Faecal metabolome and its determinants in inflammatory bowel disease. *Gut.* 2023;72:1472–85.
11. Ding NS, McDonald JAK, Perdones-Montero A, Rees DN, Adegbola SO, Misra R, Hendy P, Penez L, Marchesi JR, Holmes E, et al. Metabonomics and the gut microbiome associated with primary response to anti-TNF therapy in Crohn's disease. *J Crohns Colitis.* 2020;14:1090–102.
12. Duboc H, Rajca S, Rainteau D, Benarous D, Maubert MA, Quervain E, Thomas G, Barbu V, Humbert L, Despras G, et al. Connecting dysbiosis, bile-acid dysmetabolism and gut inflammation in inflammatory bowel diseases. *Gut.* 2013;62:531–9.
13. Hu H, Shao W, Liu Q, Liu N, Wang Q, Xu J, Zhang X, Weng Z, Lu Q, Jiao L, et al. Gut microbiota promotes cholesterol gallstone formation by modulating bile acid composition and biliary cholesterol secretion. *Nat Commun.* 2022;13:252.
14. Sinha SR, Haileselassie Y, Nguyen LP, Tropini C, Wang M, Becker LS, Sim D, Jarr K, Spear ET, Singh G, et al. Dysbiosis-induced secondary bile acid deficiency promotes intestinal inflammation. *Cell Host Microbe.* 2020;27(659–670): e655.
15. Van den Bossche L, Hindryckx P, Devisscher L, Devriese S, Van Welden S, Holvoet T, Vilchez-Vargas R, Vital M, Pieper DH, Vandenberghe J, et al. Ursodeoxycholic acid and its taurine- or glycine-conjugated species reduce colitogenic dysbiosis and equally suppress experimental colitis in mice. *Appl Environ Microbiol.* 2017;83:e02766–e2816.
16. He Z, Ma Y, Yang S, Zhang S, Liu S, Xiao J, Wang Y, Wang W, Yang H, Li S, Cao Z. Gut microbiota-derived ursodeoxycholic acid from neonatal dairy calves improves intestinal homeostasis and colitis to attenuate extended-spectrum beta-lactamase-producing enteroaggregative *Escherichia coli* infection. *Microbiome.* 2022;10:79.
17. Han B, Lv X, Liu G, Li S, Fan J, Chen L, Huang Z, Lin G, Xu X, Huang Z, et al. Gut microbiota-related bile acid metabolism-FXR/TGR5 axis impacts the response to anti-alpha4beta7-integrin therapy in humanized mice with colitis. *Gut Microbes.* 2023;15:2232143.
18. Huang L, Zheng J, Sun G, Yang H, Sun X, Yao X, Lin A, Liu H. 5-Aminosalicylic acid ameliorates dextran sulfate sodium-induced colitis in mice by modulating gut microbiota and bile acid metabolism. *Cell Mol Life Sci.* 2022;79:460.
19. Yu Z, Li D, Sun H. Herba *Origani* alleviated DSS-induced ulcerative colitis in mice through remodeling gut microbiota to regulate bile acid and short-chain fatty acid metabolisms. *Biomed Pharmacother.* 2023;161: 114409.
20. Dong S, Zhu M, Wang K, Zhao X, Hu L, Jing W, Lu H, Wang S. Dihydromyricetin improves DSS-induced colitis in mice via modulation of fecal-bacteria-related bile acid metabolism. *Pharmacol Res.* 2021;171: 105767.
21. Amaral JD, Viana RJ, Ramalho RM, Steer CJ, Rodrigues CM. Bile acids: regulation of apoptosis by ursodeoxycholic acid. *J Lipid Res.* 2009;50:1721–34.
22. Zhou C, Wang Y, Li C, Xie Z, Dai L. Amelioration of colitis by a gut bacterial consortium producing anti-inflammatory secondary bile acids. *Microbiol Spectr.* 2023;11: e0333022.
23. Sandborn WJ, Feagan BG, Hanauer S, Vermeire S, Ghosh S, Liu WJ, Petersen A, Charles L, Huang V, Usiskin K, et al. Long-term efficacy and safety of ozanimod in moderately to severely active ulcerative colitis: results from the open-label extension of the randomized, phase 2 TOUCHSTONE study. *J Crohns Colitis.* 2021;15:1120–9.
24. D'Haens G, Panaccione R, Baert F, Bossuyt P, Colombel JF, Danese S, Dubinsky M, Feagan BG, Hisamatsu T, Lim A, et al. Risankizumab as induction therapy for Crohn's disease: results from the phase 3 ADVANCE and MOTIVATE induction trials. *Lancet.* 2022;399:2015–30.
25. Maaser C, Sturm A, Vavricka SR, Kucharzik T, Fiorino G, Annese V, Calabrese E, Baumgart DC, Bettenworth D, Borralho Nunes P, et al. ECCO-ESGAR guideline for diagnostic assessment in IBD part 1: initial diagnosis, monitoring of known IBD, detection of complications. *J Crohns Colitis.* 2019;13:144–64.
26. Li Y, Liu M, Liu H, Sui X, Liu Y, Wei X, Liu C, Cheng Y, Ye W, Gao B, et al. The anti-inflammatory effect and mucosal barrier protection of *Clostridium butyricum* RH2 in ceftriaxone-induced intestinal dysbiosis. *Front Cell Infect Microbiol.* 2021;11: 647048.
27. Keogh CE, Kim DHJ, Pusceddu MM, Knotts TA, Rabasa G, Sladek JA, Hsieh MT, Honeycutt M, Brust-Mascher I, Barboza M, Gareau MG. Myelin as a regulator of development of the microbiota-gut-brain axis. *Brain Behav Immun.* 2021;91:437–50.
28. Chiang SR, Chuang YC, Tang HJ, Chen CC, Chen CH, Lee NY, Chou CH, Ko WC. Intratracheal colistin sulfate for BALB/c mice with early pneumonia caused by carbapenem-resistant *Acinetobacter baumannii*. *Crit Care Med.* 2009;37:2590–5.
29. Sann H, Erichsen J, Hessmann M, Pahl A, Hoffmeyer A. Efficacy of drugs used in the treatment of IBD and combinations thereof in acute DSS-induced colitis in mice. *Life Sci.* 2013;92:708–18.
30. Chen L, Li J, Ye Z, Sun B, Wang L, Chen Y, Han J, Yu M, Wang Y, Zhou Q, et al. Anti-high mobility group box 1 neutralizing-antibody ameliorates dextran sodium sulfate colitis in mice. *Front Immunol.* 2020;11: 585094.
31. Mullish BH, McDonald JAK, Pechlivanis A, Allegretti JR, Kao D, Barker GF, Kapila D, Petrof EO, Joyce SA, Gahan CGM, et al. Microbial bile salt hydrolases mediate the efficacy of faecal microbiota transplant in the treatment of recurrent *Clostridioides difficile* infection. *Gut.* 2019;68:1791–800.
32. Biancolillo A, Reale S, Foschi M, Bertini E, Antonelli L, D'Archivio AA. Characterization and authentication of "Ricotta" whey cheeses through GC-FID analysis of fatty acid profile and chemometrics. *Molecules.* 2022;27:7401.
33. Thomas JP, Modos D, Rushbrook SM, Powell N, Korcsmaros T. The emerging role of bile acids in the pathogenesis of inflammatory bowel disease. *Front Immunol.* 2022;13: 829525.
34. Chen L, Jiao T, Liu W, Luo Y, Wang J, Guo X, Tong X, Lin Z, Sun C, Wang K, et al. Hepatic cytochrome P450 8B1 and cholic acid potentiate intestinal epithelial injury in colitis by suppressing intestinal stem cell renewal. *Cell Stem Cell.* 2022;29(1366–1381): e1369.
35. Ward JBJ, Lajczak NK, Kelly OB, O'Dwyer AM, Giddam AK, Ni Gabhann J, Franco P, Tambuwala MM, Jefferies CA, Keely S, et al. Ursodeoxycholic acid and lithocholic acid exert anti-inflammatory actions in the colon. *Am J Physiol Gastrointest Liver Physiol.* 2017;312:G550–8.
36. Rao YP, Stravitz RT, Vlahcevic ZR, Gurley EC, Sando JJ, Hylemon PB. Activation of protein kinase C alpha and delta by bile acids: correlation with bile acid structure and diacylglycerol formation. *J Lipid Res.* 1997;38:2446–54.
37. Mencarelli A, Renga B, Migliorati M, Cipriani S, Distrutti E, Santucci L, Fiorucci S. The bile acid sensor farnesoid X receptor is a modulator of liver immunity in a rodent model of acute hepatitis. *J Immunol.* 2009;183:6657–66.
38. Yang H, Zhou H, Zhuang L, Auwerx J, Schoonjans K, Wang X, Feng C, Lu L. Plasma membrane-bound G protein-coupled bile acid receptor attenuates liver ischemia/reperfusion injury via the inhibition of toll-like receptor 4 signaling in mice. *Liver Transpl.* 2017;23:63–74.
39. Chen T, Huang Z, Liu R, Yang J, Hylemon PB, Zhou H. Sphingosine-1 phosphate promotes intestinal epithelial cell proliferation via S1PR2. *Front Biosci (Landmark Ed).* 2017;22:596–608.
40. Chen T, Gu K, Lin R, Liu Y, Shan Y. The function of Sphingosine-1-phosphate receptor 2 (S1PR2) in maintaining intestinal barrier and inducing ulcerative colitis. *Bioengineered.* 2022;13:13703–17.
41. Knights D, Lassen KG, Xavier RJ. Advances in inflammatory bowel disease pathogenesis: linking host genetics and the microbiome. *Gut.* 2013;62:1505–10.
42. Lewis JD, Chen EZ, Baldassano RN, Otley AR, Griffiths AM, Lee D, Bittering K, Bailey A, Friedman ES, Hoffmann C, et al. Inflammation, antibiotics, and diet as environmental stressors of the gut microbiome in pediatric Crohn's disease. *Cell Host Microbe.* 2015;18:489–500.
43. Zeng Z, Jiang M, Li X, Yuan J, Zhang H. Precision medicine in inflammatory bowel disease. *Precis Clin Med.* 2023;6:pbad033.
44. Delday M, Mulder I, Logan ET, Grant G. Bacteroides thetaiotaomicron ameliorates colon inflammation in preclinical models of Crohn's disease. *Inflamm Bowel Dis.* 2019;25:85–96.
45. Liu Y, Wang Y, Ni Y, Cheung CKY, Lam KSL, Wang Y, Xia Z, Ye D, Guo J, Tse MA, et al. Gut microbiome fermentation determines the efficacy of exercise for diabetes prevention. *Cell Metab.* 2020;31(77–91): e75.

46. Ryvchin R, Dubinsky V, Rabinowitz K, Wasserberg N, Dotan I, Gophna U. Alteration in urease-producing bacteria in the gut microbiomes of patients with inflammatory bowel diseases. *J Crohns Colitis*. 2021;15:2066–77.
47. Panpetch W, Hiengrach P, Nilgate S, Tumwasorn S, Somboonna N, Wilantho A, Chatthanathon P, Prueksapanich P, Leelahavanichkul A. Additional *Candida albicans* administration enhances the severity of dextran sulfate solution induced colitis mouse model through leaky gut-enhanced systemic inflammation and gut-dysbiosis but attenuated by *Lactobacillus rhamnosus* L34. *Gut Microbes*. 2020;11:465–80.
48. Mirsepasi-Lauridsen HC, Vallance BA, Krogfelt KA, Petersen AM. *Escherichia coli* pathobionts associated with inflammatory bowel disease. *Clin Microbiol Rev*. 2019;32:e00060–e118.
49. Lu Q, Yang MF, Liang YJ, Xu J, Xu HM, Nie YQ, Wang LS, Yao J, Li DF. Immunology of inflammatory bowel disease: molecular mechanisms and therapeutics. *J Inflamm Res*. 2022;15:1825–44.
50. Leibovitz H, Lee SH, Xue M, Raygoza Garay JA, Hernandez-Rocha C, Madson KL, Meddings JB, Guttman DS, Espin-Garcia O, Smith MI, et al. Altered gut microbiome composition and function are associated with gut barrier dysfunction in healthy relatives of patients with Crohn's disease. *Gastroenterology*. 2022;163(1364–1376): e1310.
51. Teofani A, Marafini I, Laudisi F, Pietrucci D, Salvatori S, Unida V, Biocca S, Monteleone G, Desideri A. Intestinal taxa abundance and diversity in inflammatory bowel disease patients: an analysis including covariates and confounders. *Nutrients*. 2022;14:260.
52. Ruigrok R, Collij V, Sureda P, Klaassen MAY, Bolte LA, Jansen BH, Voskuil MD, Fu J, Wijmenga C, Zhernakova A, et al. The composition and metabolic potential of the human small intestinal microbiota within the context of inflammatory bowel disease. *J Crohns Colitis*. 2021;15:1326–38.
53. Xiao F, Dong F, Li X, Li Y, Yu G, Liu Z, Wang Y, Zhang T. *Bifidobacterium longum* CECT 7894 improves the efficacy of infliximab for DSS-induced colitis via regulating the gut microbiota and bile acid metabolism. *Front Pharmacol*. 2022;13: 902337.
54. Elinav E, Strowig T, Kau AL, Henao-Mejia J, Thaiss CA, Booth CJ, Peaper DR, Bertin J, Eisenbarth SC, Gordon JI, Flavell RA. NLRP6 inflammasome regulates colonic microbial ecology and risk for colitis. *Cell*. 2011;145:745–57.
55. Choi H, Bae SJ, Choi G, Lee H, Son T, Kim JG, An S, Lee HS, Seo JH, Kwon HB, et al. *Ninjurin1* deficiency aggravates colitis development by promoting M1 macrophage polarization and inducing microbial imbalance. *FASEB J*. 2020;34:8702–20.
56. Liu B, Piao X, Niu W, Zhang Q, Ma C, Wu T, Gu Q, Cui T, Li S. *Kujijieyuan* decoction improved intestinal barrier injury of ulcerative colitis by affecting TLR4-dependent PI3K/AKT/NF-kappaB oxidative and inflammatory signaling and gut microbiota. *Front Pharmacol*. 2020;11:1036.
57. Xu HM, Huang HL, Liu YD, Zhu JQ, Zhou YL, Chen HT, Xu J, Zhao HL, Guo X, Shi W, et al. Selection strategy of dextran sulfate sodium-induced acute or chronic colitis mouse models based on gut microbial profile. *BMC Microbiol*. 2021;21:279.
58. Kwan SY, Jiao J, Qi J, Wang Y, Wei P, McCormick JB, Fisher-Hoch SP, Beretta L. Bile acid changes associated with liver fibrosis and steatosis in the Mexican-American population of south Texas. *Hepatol Commun*. 2020;4:555–68.
59. Chen SY, Shen YC, Lin JA, Yen GC. *Rhinacanthus nasutus* and okara polysaccharides attenuate colitis via inhibiting inflammation and modulating the gut microbiota. *Phytother Res*. 2022;36:4631–45.
60. Zhou Y, Li R, Zheng Y, Song M, Zhang S, Sun Y, Wei M, Fan X. *Diosgenin* ameliorates non-alcoholic fatty liver disease by modulating the gut microbiota and related lipid/amino acid metabolism in high fat diet-fed rats. *Front Pharmacol*. 2022;13: 854790.

Publisher's Note

Springer Nature remains neutral with regard to jurisdictional claims in published maps and institutional affiliations.